Isothermal Crystallization Behavior of Poly(L-lactide) in Poly(L-lactide)-*block*-Poly(ethylene glycol) Diblock Copolymers

CHING-I HUANG,[1] SHANG-HSIU TSAI,[2] CHIH-MING CHEN[1]

[1]Institute of Polymer Science and Engineering, National Taiwan University, Taipei 106, Taiwan

[2]Institute of Materials Science and Technology, National Taiwan University of Science and Technology, Taipei 106, Taiwan

Received 11 January 2006; revised 3 May 2006; accepted 28 May 2006
DOI: 10.1002/polb.20890
Published online in Wiley InterScience (www.interscience.wiley.com).

ABSTRACT: The crystal unit-cell structures and the isothermal crystallization kinetics of poly(L-lactide) in biodegradable poly(L-lactide)-*block*-methoxy poly(ethylene glycol) (PLLA-*b*-MePEG) diblock copolymers have been analyzed by wide-angle X-ray diffraction and differential scanning calorimetry. In particular, the effects due to the presence of MePEG that is chemically connected to PLLA as well as the PLLA crystallization temperature T_C are examined. Though we observe no variation of both the PLLA and MePEG crystal unit-cell structures with the block ratio between PLLA and MePEG and T_C, the isothermal crystallization kinetics of PLLA is greatly influenced by the presence of MePEG that is connected to it. In particular, the equilibrium melting temperature of PLLA, $T^o_{m,PLLA}$, significantly decreases in the diblock copolymers. When the T_C is high so that the crystallization is controlled by nucleation, because of the decreasing $T^o_{m,PLLA}$ and thereafter the nucleation density with decreasing PLLA molecular weight, the crystallinity of PLLA also decreases with a decrease in the PLLA molecular weight. While, for the lower crystallization temperature regime controlled by the growth mechanism, the crystallizability of PLLA in copolymers is greater than that of pure PLLA. This suggests that the activation energy for the PLLA segment diffusing to the crystallization site decreases in the diblocks. © 2006 Wiley Periodicals, Inc. J Polym Sci Part B: Polym Phys 44: 2438–2448, 2006
Keywords: block copolymers; crystallization; poly(L-lactide)

INTRODUCTION

Biodegradable block copolymers continue to attract a lot of attention because of their numerous biomedical applications.[1–3] Much of the research has focused on the synthesis as well as the available applications. Although there have been recently a few studies in discussing the crystallization behavior and structure development,[4–15] the crystallization kinetics in crystalline–crystalline biodegradable block copolymers has not been well understood. Thus, we adopt a type of self-synthesized crystalline–crystalline diblock biocopolymers to systematically analyze the crystallization kinetics during the isothermal crystallization processes.

We consider poly(L-lactide)-*block*-monomethoxy poly(ethylene glycol) (PLLA-*b*-MePEG) diblock copolymers. PLLA and PEG are known to be biocompatible. Their block copolymers have been proposed for a wide range of medical applications

Correspondence to: C.-I. Huang (E-mail: chingih@ntu.edu.tw)

Journal of Polymer Science: Part B: Polymer Physics, Vol. 44, 2438–2448 (2006)

due to drug permeability and degradability.[1,16] So far, most studies related to PLLA-PEG block copolymers have focused on the synthesis and the thermal crystallization behavior, which are primarily based on the nuclear magnetic resonance (NMR), differential scanning calorimeter (DSC), and wide-angle X-ray diffraction (WAXD) measurements.[4,6–7,11,13,14,17–20] For example, Kim et al.[6] investigated the variation of the crystal structure and crystallization behavior with the block ratio in the PLLA-PEG diblock and triblock copolymers by WAXD and DSC experiments. They found that the crystal unit-cell structures of both PLLA and PEG are independent of the block length and the crystallization temperature. However, the crystallization of the PLLA block is retarded by the presence of the PEG block. Sun et al.[13] synthesized a series of PLLA-MePEG block copolymers with identical MePEG molecular weight but various PLLA molecular weights. From the DSC experiments, they observed that with increasing the molecular weight of PLLA in the copolymers, the melting point of PLLA increases, but the melting point of MePEG tends to decrease. This phenomenon indicates that the crystallization of both components is greatly influenced by the presence of the other component. In addition, by comparing the nonisothermal crystallization behavior of PLLA-PEO-PLLA triblock copolymers with the same composition of binary PLLA and PEO blends, Shin et al.[14] observed that the chain connectivity in the triblock copolymer can reduce the chain mobility and the crystallization of each component thus decreases. Also, they observed that the degree of optical retardation due to the crystallization of PEO was greater in the triblock copolymer. It should be noted that although both Kim et al.[6] and Shin et al.[14] reported the effects of the connected PEG block on the crystallizability of PLLA, they did not analyze the crystallization behavior in a wide range of the crystallization temperature.

In this article, we study the isothermal crystallization kinetics of PLLA as well as the crystal unit-cell structures in the PLLA-MePEG diblock copolymers by DSC and WAXD techniques. To our knowledge, there have been extensive studies that have focused on the crystallization kinetics of pure PLLA.[21–28] However, there exist few studies on the PLLA crystallization kinetics in the presence of MePEG that is chemically connected to it. We therefore synthesize a series of PLLA-MePEG block copolymers with the same MePEG molecular weight but various PLLA molecular weights. PLLA and PEG are reported to be miscible in the melt.[22] The melting temperatures of PLLA and MePEG are around 150–190 °C and 60 °C, respectively.[29] As such, when the samples are first melted at 200 °C and then quenched to $T_C \geq 70$ °C, we expect that only PLLA component can crystallize in the presence of amorphous MePEG block from a homogeneous melt state. We then examine the effects of the connected MePEG block on the formation of PLLA crystals and the crystallization behavior of PLLA at various temperatures T_C. From the WAXD analysis, the crystal unit-cell structure parameters as a function of T_C and the block ratio between PLLA and MePEG are studied. With the aid of DSC, we examine the melting temperature and the crystallinity of PLLA as a function of PLLA molecular weight and crystallization temperature. We also analyze the relative crystallinity of PLLA as a function of time via the Avrami equation, from which the crystallization growth rate of PLLA at a given T_C is obtained.

EXPERIMENTAL

Materials and Synthesis

PLLA-MePEG diblock copolymers were synthesized by a ring-opening polymerization. L-lactide (Tokyo Kasei Kogyo) was purified by recrystallization in ethyl acetate. The monomethoxy-terminated poly(ethylene glycol) (MePEG) with the number-average molecular weight $M_n = 5000$ was purchased from Aldrich. First, a certain weight ratio of L-lactide and MePEG (shown in Table 1) was put into a dry tristoppered flask with stirring. The flask was purged with nitrogen and placed in a silicone oil bath at 110 °C. After the mixture was fully melted, a few amount of the stannous octoate (1% of PLLA weight) was introduced to serve as the catalyst. The system was continuously purged with nitrogen and the temperature was raised up to 130 °C to proceed the ring-opening polymerization for 24 h. The reaction product was then dissolved in chloroform with stirring for 2–3 h at room temperature, and precipitated by a mixture of *n*-hexane and methyl alcohol under an ice bath. The above purification process (dissolution/precipitation) was carried out for four times. The precipitate was finally filtered and

Table 1. Sample Characteristics of PLLA Homopolymer and PLLA–MePEG Diblock Copolymers

Samples	L-Lactide Content in the Feed (wt %)	N_{PLLA}	N_{MePEG}	f_{PLLA}	M_n	Polydispersity[a]
PLLA	100	283		1	20,400[a]	1.6
PLLA-61	74	181	114	0.61	18,000	1.1
PLLA-43	58	86	114	0.43	11200	1.1
PLLA-33	48	56	114	0.33	9000	1.2

[a] Determined by GPC.

dried under vacuum at 45 °C for 3 days. For the sake of comparison, PLLA homopolymer has been synthesized as well.

We employed ^{1}H NMR (Jeol EX-400, deuterated chloroform) to determine the PLLA composition in the copolymer, f_{PLLA}, which is equal to $N_{PLLA}/(N_{PLLA} + N_{MePEG})$ with N_I = degree of polymerization of component I. The molecular weights of the samples were then obtained based on f_{PLLA} and the fixed number-average molecular weight of MePEG (M_n = 5000). With the aid of gel permeation chromatography (GPC; PLgel, 5 μm Mixed-C, Polymer Laboratories), we determined the polydispersity of the samples. Tetrahydrofuran (THF) was used as the evoluting solvent at a rate of 0.8 mL/min. Polystyrene (M_n = 580–377400) was used as a standard. Finally, we listed the characteristics of the PLLA-MePEG diblock copolymers and PLLA homopolymer used in this study in Table 1.

Wide-Angle X-ray Diffraction (WAXD)

The samples were first heated to 200 °C in the air oven for 10 min annealing, and then rapidly transferred to another air oven preheated to the desired crystallization temperate (T_C) $\geq$70 °C for 24 h in order for PLLA to crystallize completely. Finally, the specimens were moved out from the oven to room temperature around 25 °C so that MePEG can crystallize in the matrix of PLLA crystalline domains. WAXD experiments were carried out on the samples with a Rigaku Denki diffractometer with Cu Kα radiation (λ = 1.542 Å) at a scanning rate of 2° θ/min, where θ is the scattering angle (the angle between the incident X-ray beam and the scattered X-ray beam). The accelerating voltage was 40 kV, and the tube current was 100 mA. The X-rays were monochromated with a graphite. All measurements were performed at room temperature in the air.

Differential Scanning Calorimeter (DSC)

The kinetics of isothermal crystallization of PLLA homopolymer and PLLA-MePEG diblock copolymers were analyzed by a PerkinElmer DSC-7 differential scanning calorimeter in a nitrogen purge. First, the samples were heated from room temperature to 200 °C and annealed for 10 min in the melt to remove the thermal history. The samples were then quickly quenched to the desired crystallization temperature (T_C) $\geq$70 °C at a cooling rate of 100 °C/min, and kept at this temperature to the end of the exothermic PLLA crystallization peak. The heat flow per gram of the sample evolved during the isothermal crystallization process was recorded as a function of time, from which the overall PLLA crystallinity and the relative crystallinity of PLLA are obtained.

After complete crystallization of PLLA during the isothermal crystallization, the samples were heated from the crystallization temperature to a melt with a heating rate of 10 °C/min. The heat flow per gram of the sample evolved during the scanning process was measured as a function of temperature, from which the melting temperature of PLLA was determined from the maxima.

RESULTS AND DISCUSSION

WAXD Analysis

We employ WAXD to examine the unit-cell structures of both crystalline PLLA and MePEG components for a series of PLLA-MePEG diblock copolymers (PLLA-61, PLLA-43, and PLLA-33), which are first isothermally crystallized at vari-

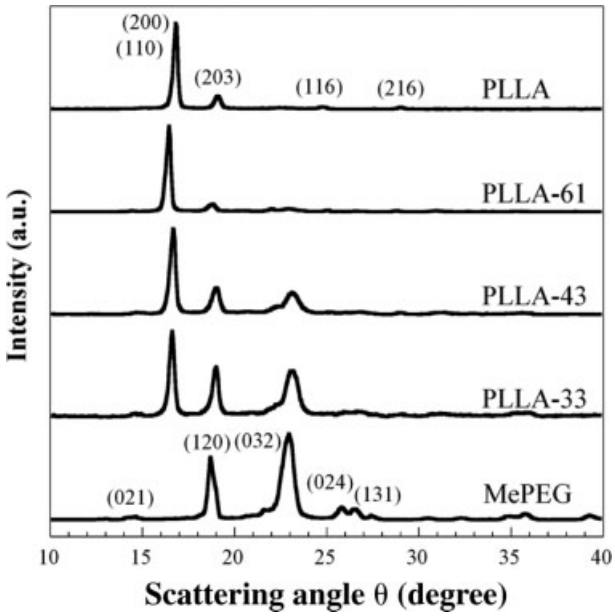

Figure 1. WAXD patterns in terms of the intensity and scattering angle (θ) for each diblock sample is first isothermally crystallized at T_C = 100 °C for PLLA crystallization and then quenched to 25 °C for MePEG crystallization. In a comparison, the WAXD patterns for pure PLLA and MePEG crystallized at 100 and 25 °C, respectively, are also shown.

ous T_C between 70 and 130 °C for PLLA crystallization and then quenched to 25 °C for MePEG crystallization. For a comparison, we also examine the WAXD results for pure PLLA crystallized at various T_C and for pure MePEG crystallized at 25 °C. Typical WAXD patterns in terms of Intensity (I) and scattering angle (θ) for each sample are shown in Figure 1, where PLLA component is crystallized at T_C = 100 °C and MePEG at 25 °C. As denoted in Figure 1, the main peak positions as well as their corresponding (hkl) reflection planes from pure PLLA and pure MePEG are consistent with those from refs. 30 and 31, respectively, indicating that PLLA and MePEG belong to the orthorhombic and monoclinic crystal system, respectively. In further, the peak positions from the WAXD profiles for each diblock sample are a superposition of the peak positions from pure PLLA and pure MePEG, respectively, which reveals that each crystallizable component in the diblocks forms a similar unit-cell structure as the pure component.

The unit-cell structure parameters (a, b, c) are easily determined through the insertion of the values of λ (1.542 Å) and the main peak positions of the reflection planes into the form of the interplanar spacing of the (hkl) reflection planes, which is given by

$$\left(\frac{1}{d_{hkl}}\right)^2 = \left(\frac{2\sin(\theta_{hkl}/2)}{\lambda}\right)^2 = \frac{h^2}{a^2} + \frac{k^2}{b^2} + \frac{l^2}{c^2} \quad (1a)$$

for PLLA belonging to the orthorhombic system, and

$$\left(\frac{1}{d_{hkl}}\right)^2 = \left(\frac{2\sin(\theta_{hkl}/2)}{\lambda}\right)^2 = \frac{1}{\sin^2\beta}\left(\frac{h^2}{a^2} + \frac{k^2\sin^2\beta}{b^2} + \frac{l^2}{c^2} - \frac{2hl\cos\beta}{ac}\right) \quad (1b)$$

for MePEG belonging to the monoclinic system. In eq 1b, the value of β is equal to 125.4°.[31] We find that the unit-cell parameters of both PLLA and MePEG in each diblock sample do not change with the earlier crystallization temperature of PLLA, T_C, indicating that not only the PLLA crystal unit-cell parameters remain the same with T_C, but also there are no distortions of the MePEG crystal structures due to the presence of the earlier PLLA crystalline domains at T_C. We thus average these unit-cell parameters for the diblocks as well as for pure PLLA and pure MePEG, and list them in Table 2. As can be seen clearly, the unit-cell parameters for each diblock sample are almost identical to those for pure components,[6] which also agree well with the reported values.[30,31] That is, the formation of the PLLA and MePEG crystal unit-cell structures is not affected by the chain-connectivity as well as the block ratio between PLLA and MePEG.

Table 2. Unit-Cell Structure Parameters of PLLA and MePEG Crystals for the Diblock Copolymer Samples and Pure PLLA and MePEG[a]

	PLLA			MePEG		
Samples	a (Å)	b (Å)	c (Å)	a (Å)	b (Å)	c (Å)
PLLA	10.56	6.05	28.90			
PLLA-61	10.71	6.12	28.61	8.29	12.92	20.76
PLLA-43	10.73	6.19	27.93	8.35	13.04	20.94
PLLA-33	10.79	6.18	28.36	8.35	13.00	20.83
MePEG				8.24	13.36	18.59

[a] Determined by averaging the parameters for systems first isothermally crystallized at T_C = 70, 80, 90, 100, 110, 120, and 130 °C, respectively, for PLLA crystallization and then quenched to 25 °C for MePEG crystallization.

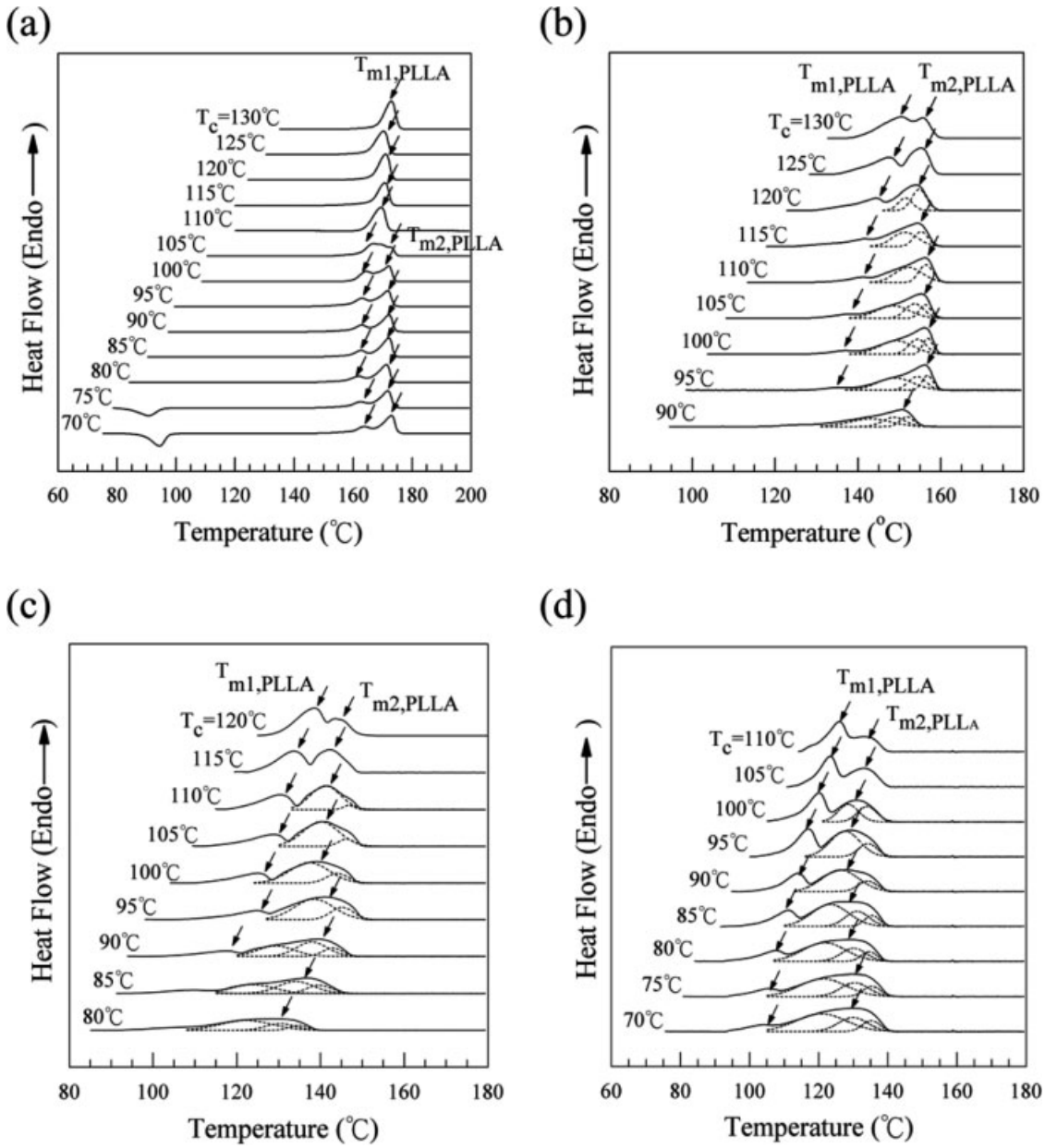

Figure 2. DSC melting endotherms of (a) pure PLLA, (b) PLLA-61, (c) PLLA-43, and (d) PLLA-33 with a heating rate of 10 °C/min after isothermal crystallization at various temperatures T_C. The dashed curves represent the Gaussian peaks from the deconvolution of the higher melting temperature peak $T_{m2,PLLA}$.

DSC Analysis

Melting Behavior

Figure 2(a–d) present the DSC melting endotherms of pure PLLA, PLLA-61, PLLA-43, and PLLA-33, respectively, first allowing PLLA component to isothermally crystallize at various $T_C \leq 70$ °C from a homogeneous melt state at 200 °C, and then heated at a rate of 10 °C/min. For neat PLLA, it is evident that two melting temperature peaks for the PLLA component, $T_{m1,PLLA}$ and $T_{m2,PLLA}$, as indicated by arrows in Figure 2(a), are observed when $T_C \leq 105$ °C. As can be seen clearly, $T_{m2,PLLA}$ is independent of T_C, and even disappears when T_C increases to be greater than 105 °C. The value of $T_{m1,PLLA}$, which is plotted as a function of T_C in Figure 3, is observed to be linearly increasing with T_C

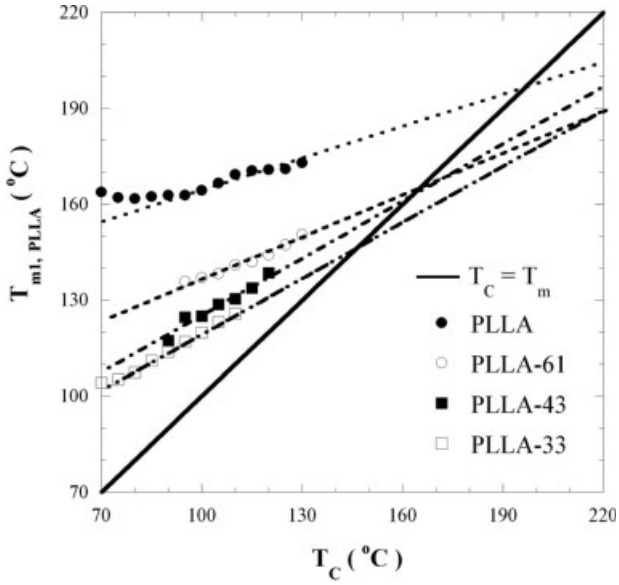

Figure 3. Variation of $T_{m1,PLLA}$ with T_C for neat PLLA and diblock samples PLLA-61, PLLA-43, and PLLA-33.

when T_C is higher than 95 °C. By extrapolating the line of $T_{m1,PLLA}$ versus T_C to the line $T_m = T_C$ according to the linear Hoffman–Weeks analysis,[32] we obtain the equilibrium melting temperature of PLLA, $T^o_{m,PLLA}$, which is around 196 °C. This result is in a good agreement with ref. 22, but comes with a difference of 10 °C compared with the value of $T^o_{m,PLLA}$ equal to 206 °C listed in the literature.[21,23] We believe this is due to the difference of the molecular weight of PLLA. As such, the equilibrium thickness of the crystallites as well as the equilibrium melting temperature varies. The existence of double melting peaks in the DSC heating profiles of pure PLLA may result from one of the following reasons: the presence of two different crystal structures, the presence of two different thicknesses of crystal lamellae with the same type of crystal structure formed at the isothermal crystallization conditions,[33] and the simultaneous melting-reorganization/recrystallization-remelting of the lamellae originally formed during the crystallization process.[34] Our previous WAXD results have shown that only one unit-cell structure of PLLA crystals forms during the crystallization process. Thus, the occurrence of the double melting peaks is mainly caused by the existence of the single type of crystal unit-cell structure but with different crystal thicknesses. Are these two different thicknesses of crystals formed at the beginning of the isothermal crystallization process or at the later heating process due to the reorganization and/or the recrystallization of the original lamellar stacks? As illustrated in Figure 2(a), the lower melting temperature peak $T_{m1,PLLA}$ becomes more obvious; while the higher peak $T_{m2,PLLA}$ gradually decreases as the crystallization temperature T_C increases. Furthermore, $T_{m2,PLLA}$ even disappears when T_C is above 105 °C. Moreover, $T_{m2,PLLA}$ also disappears with an increase in the heating rate. Recall that at higher crystallization temperatures, it is easier to form more perfect and larger crystal lamellae, and therefore it is more difficult for the reorganization and/or the recrystallization process to occur. Also, when the heating rate is too fast, there is no sufficient time for the original lamellar stacks to undergo the reorganization and/or the recrystallization process. As such, the fact that the higher melting peak $T_{m2,PLLA}$ does not exist in the DSC melting endotherms at high crystallization temperature and/or heating rate indicates that $T_{m2,PLLA}$ is a result of the melting of the crystallites recrystallized during the heating process, while the lower melting peak $T_{m1,PLLA}$ refers to the melting of the primary crystallites formed during the isothermal crystallization process.

Similar to the melting behavior of pure PLLA crystallization, two apparent melting temperature peaks for the PLLA component, $T_{m1,PLLA}$ and $T_{m2,PLLA}$, are also observed in the diblocks PLLA-61, PLLA-43, and PLLA-33, shown in Figure 2(b–d), respectively. However, the higher melting temperature peak $T_{m2,PLLA}$ becomes broader and can be separated into three Gaussian peaks at lower isothermal crystallization temperature T_C. These three peaks emerge to become two peaks or even one peak as T_C increases. In further, the peak area around $T_{m2,PLLA}$ decreases with increasing T_C. Hence, the occurrence of $T_{m2,PLLA}$ may also result from the melting of the crystallites recrystallized during the heating process. While, the lower peak $T_{m1,PLLA}$, which increases with increasing T_C, is due to the melting of the original crystallites formed during the isothermal crystallization process. To obtain the equilibrium melting temperature of PLLA for each block copolymer sample, we also plot the values of $T_{m1,PLLA}$ versus T_C for PLLA-61, PLLA-43, and PLLA-33 in Figure 3. As analyzed in pure PLLA, we obtain the value of $T^o_{m,PLLA}$, for PLLA-61, PLLA-43, and PLLA-33, equal to around 165, 162, and 147 °C, respectively. This result shows a trend that the $T^o_{m,PLLA}$ value in

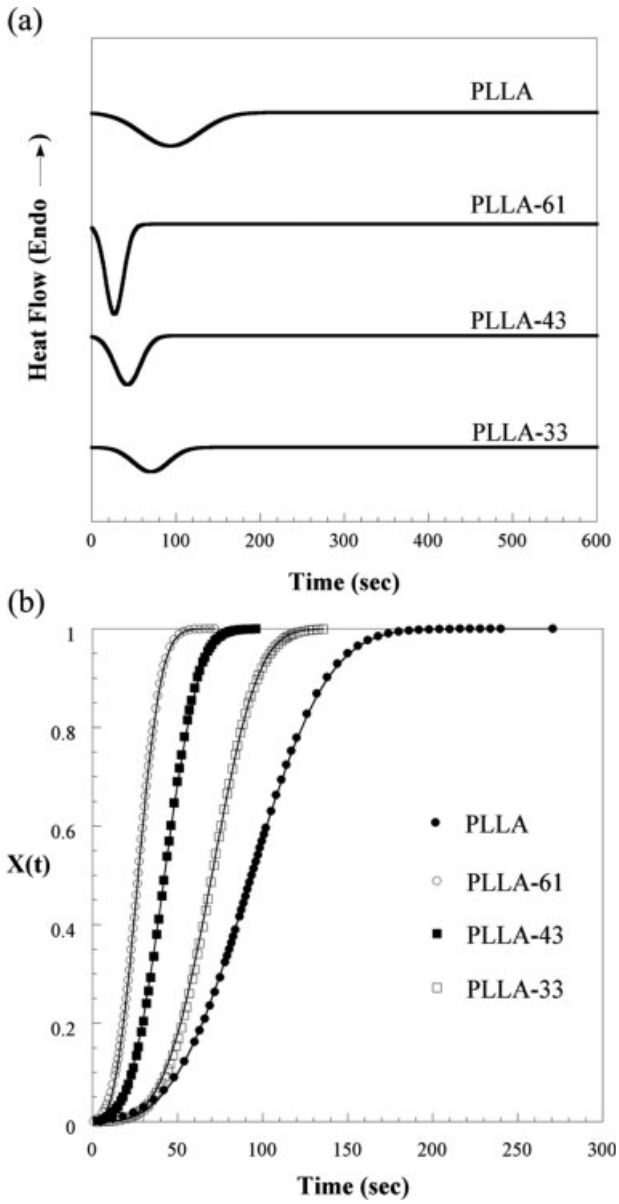

Figure 4. (a) DSC exothermic curves and (b) PLLA relative crystallinity versus crystallization time for various systems undergoing an isothermal crystallization process at $T_C = 90$ °C. The solid curves in (b) represent the best fit results by the Avrami equation with the values of n and k listed in Table 3.

the copolymers decreases with decreasing the PLLA molecular weight. However, compared with the value of $T^o_{m,PLLA}$ of pure PLLA, the equilibrium melting temperature of PLLA in the diblock samples decreases dramatically, suggesting that the presence of the miscible PEG blocks also has a great influence on the crystallization as well as the melting behavior of PLLA. That is, the dependence of the PLLA melting temperature in the diblock copolymers is not simply due to the variation of PLLA molecular weight. The dilution effect caused by the miscible MePEG also plays a very important role on this sharp $T^o_{m,PLLA}$ decreasing behavior.

Isothermal Crystallization Behavior

With the recorded DSC exothermic curves in terms of the heat flow per gram of the sample $dH(t)/dt$ as a function of time t for systems undergoing the isothermal PLLA crystallization process at various values of T_C, we can analyze the isothermal PLLA crystallization kinetics. First, we calculate the relative crystallinity of PLLA, $X(t)$, by the following equation

$$X(t) = \frac{\int_0^t \frac{dH(t)}{dt}\, dt}{\int_0^\infty \frac{dH(t)}{dt}\, dt} \tag{2}$$

Once the values of $X(t)$ versus t are obtained, the isothermal crystallization kinetics are interpreted in terms of the Avrami equation[35]

$$X(t) = 1 - \exp(-kt^n) \tag{3}$$

where n is known as the Avrami index, and k is the overall crystallization rate constant including contributions from nucleation and crystal growth. For example, Figure 4(a) presents the DSC exothermic curves as a function of time t for each diblock sample and pure PLLA undergoing the isothermal crystallization of PLLA at $T_C = 90$ °C, from which the values of $X(t)$ calculated by eq 2 versus t are obtained, as shown in Figure 4(b). It is clear that the fit of the Avrami equation to the experimental data of each sample crystallized at 90 °C in Figure 4(b) is remarkably good in the whole conversion range, which is also true for the systems crystallized at other values of T_C. As listed in Table 3, where we present the fitting Avrami constants n and k, most of the n values for the temperature examined here are in the range between 3 and 4, indicating that the growing of spherulites due to the crystallization of PLLA is three-dimensional. However, for the sample PLLA-33 at T_C higher than 100 °C, n deviates to a higher value 5, which may result from the presence of major amorphous MePEG domains. Thus, the growing of the ordinary PLLA spherulites is destroyed and the n value deviates from 3 to 4. Indeed, with increasing the amount of amorphous MePEG, the

Table 3. Avrami Parameters for Various Samples at T_C

Samples	T_C (°C)	n	k
PLLA	80	3.55	7.45E-10
	85	3.51	6.41E-09
	90	3.06	6.49E-07
	95	3.26	1.49E-06
	100	3.46	1.42E-06
	105	3.47	1.38E-06
	110	3.45	1.67E-06
	115	2.82	8.86E-06
	120	3.51	4.90E-08
	125	3.59	1.45E-08
	130	3.51	7.70E-09
PLLA-61	90	2.90	5.02E-05
	95	2.74	1.91E-04
	100	3.32	1.35E-05
	105	3.35	6.69E-06
	110	3.57	1.32E-06
	115	3.17	1.51E-06
	120	2.87	1.22E-06
	125	3.20	2.64E-08
	130	3.15	2.09E-09
PLLA-43	80	2.60	4.29E-05
	85	2.75	2.61E-05
	90	3.07	7.06E-06
	95	3.23	4.72E-06
	100	3.31	1.07E-06
	105	3.36	5.23E-07
	110	3.24	1.01E-07
	115	3.08	3.85E-08
	120	3.11	1.33E-09
PLLA-33	70	3.01	9.14E-06
	75	2.51	1.10E-05
	80	3.16	4.56E-06
	85	3.57	4.24E-07
	90	3.72	9.46E-08
	95	3.97	1.45E-08
	100	5.04	1.22E-11
	105	5.67	1.49E-14
	110	5.13	6.29E-15

resulting spherulites vary from ordinary to banded to dentritic (tree-like).[13]

With the values of the overall crystallization rate k determined from the Avrami analysis, the time for half of the crystallization to develop, $t_{1/2}$, is calculated by

$$t_{1/2} = \left(\frac{\ln 2}{k}\right)^{1/n} \tag{4}$$

from which the crystallization growth rate, G, defined as $G = 1/t_{1/2}$, is obtained. Figure 5 plots G versus T_C for pure PLLA, PLLA-61, PLLA-43, and PLLA-33. We observe that with increasing the crystallization temperature of PLLA for each sample, the growth rate first shows an increasing and then a decreasing behavior. This behavior has been very common due to the balance between two well-known opposing effects on the crystallization rate. As T_C decreases and approaches the glass transition temperature, T_g, the crystallization growth rate is greatly retarded by the significant decrease of the chain mobility. While when T_C is high and approaches the equilibrium melting temperature T_m^o, although the chain mobility increases, it is overcome by the great decrease of the formed nucleation density, and the crystallization rate decreases at low degrees of supercooling. As such, because of the decrease of $T_{m,PLLA}^o$ with decreasing PLLA molecular weight and/or the dilution effect caused by the miscible MePEG in the copolymers, we also observe that the crystallization temperature, at which the PLLA crystallization growth rate G reaches a maximum, shifts to a lower value with decreasing the PLLA molecular weight. In further, when the crystallization temperature is in the intermediate regime between 80 and 110 °C, the presence of a short MePEG block that is chemically connected to PLLA (such as in sample PLLA-61) causes a significant increase of the PLLA crystallization rate.

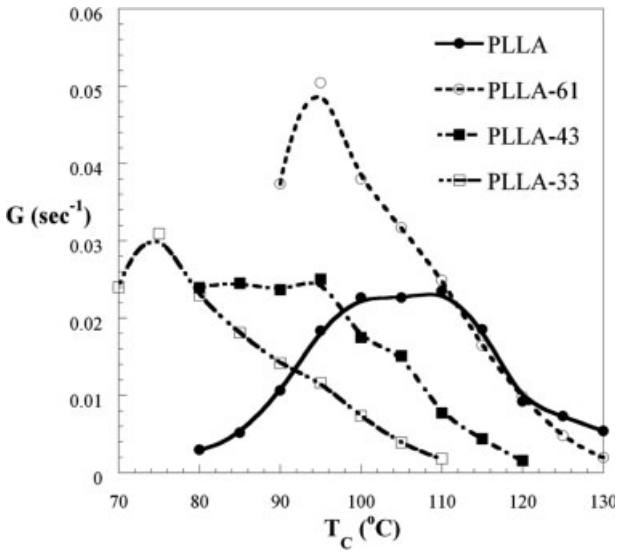

Figure 5. Plot of the PLLA crystallization growth rate G in pure PLLA, PLLA-61, PLLA-43, and PLLA-33, as a function of crystallization temperature T_C.

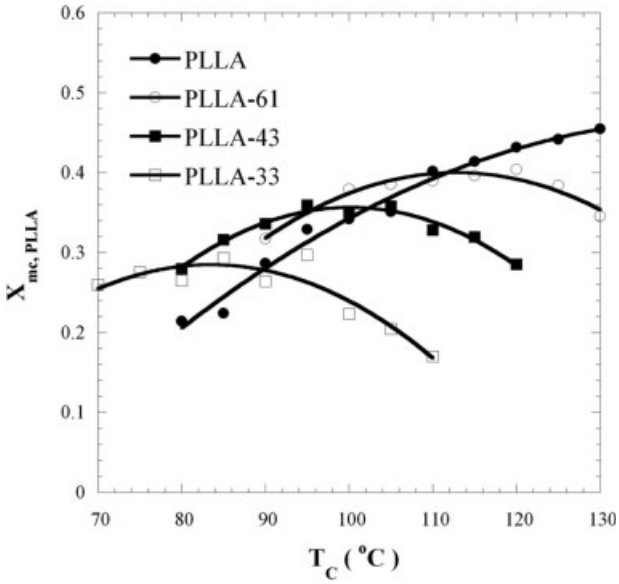

Figure 6. Plot of the normalized crystallinity of PLLA component, $X_{mc,PLLA}$, as a function of T_C for various systems isothermally crystallized at T_C from a homogeneous melt state at 200 °C.

The overall crystallinity of PLLA, $\omega_{mc,PLLA}$, at T_C can also be calculated from the isothermal DSC exothermic curves by

$$\omega_{mc,PLLA} = \frac{\Delta H}{\Delta H^{\circ}_{PLLA}} = \frac{\int_0^{\infty} \frac{dH(t)}{dt}\, dt}{\Delta H^{\circ}_{PLLA}} \qquad (5a)$$

where ΔH is the area of the exothermic PLLA crystallization peak (i.e., $\int_0^{\infty} \frac{dH(t)}{dt}\, dt$), and $\Delta H^{o}_{m,PLLA}$ is the heat of melting per gram of 100% crystalline PLLA equal to 135 J/g.[24] To examine the effects of copolymer composition on the crystallinity of PLLA, in Figure 6 we plot the normalized crystallinity of PLLA, defined as

$$X_{mc,PLLA} = \omega_{mc,PLLA}/wt_{PLLA} \qquad (5b)$$

in Figure 6. As seen in Figure 6, the crystallinity of pure PLLA increases with T_C when T_C is within 80–130 °C. However, within the same crystallization temperature regime, the normalized crystallinity of PLLA in the diblocks first shows an increasing trend with T_C and then a decreasing behavior with a further increase in T_C. The existence of such a maximum is quite reasonable for systems undergoing the crystallization with the process of nucleation and growth. That is, at low degrees of supercooling, the decreasing degree of the formed nuclei is much larger than the increasing degree of the PLLA mobility, and thus the crystallizability of PLLA decreases with T_C. However, at high degrees of supercooling, although the formed nucleation density increases, its increasing degree is still overcome by the great decrease of the mobility, and thus the crystallizability of PLLA decreases with T_C decreasing. Because decreasing PLLA molecular weight depresses the value of $T^{o}_{m,PLLA}$, the sample with lower PLLA molecular weight at the same T_C indeed undergoes a crystallization at a smaller degree of supercooling. As such, we observe that the crystallization temperature, at which the normalized PLLA crystallinity in the diblocks reaches a maximum, shifts to a lower value with decreasing the PLLA molecular weight. In a comparison of the normalized PLLA crystallinity $X_{mc,PLLA}$ between PLLA homopolymer and the diblocks at the same crystallization temperature T_C, we observe a decreasing trend of $X_{mc,PLLA}$ with pure PLLA→PLLA-61→PLLA-43→PLLA-33 when $T_C > 110$ °C. This is not surprising since $T^{o}_{m,PLLA}$ in the copolymers decreases with decreasing the PLLA molecular weight, the crystallization of PLLA with lower PLLA molecular weight at the same T_C corresponds to a lower degree of supercooling. As a result, the formed PLLA nucleation density as well as the crystallizability of PLLA decreases with decreasing the PLLA molecular weight. While, at lower crystallization temperature regime in which PLLA crystallizes according to the growth mechanism, the normalized PLLA crystallinity in the diblocks is seen to be greater than that for pure PLLA. This suggests that the presence of amorphous MePEG, which is chemically connected to PLLA indeed may promote the ability for the PLLA chains to diffuse to the crystallization sites. Thus, we may expect that the activation energy for the segment diffusing to the crystallization site decreases in the diblocks. Note that both Kim et al.[6] and Shin et al.[14] claimed that the PLLA crystallinity is reduced by the presence of PEG block and/or the connectivity between PLLA and PEG. However, they did not analyze the crystallization behavior in a wide range of the crystallization temperature. As such, they did not observe our results that the effects of the presence of MePEG blocks on the crystallizability of PLLA indeed is strongly dependent on the crystallization temperature T_C, i.e., the crystallization mechanism regime.

CONCLUSIONS

We employ WAXD and DSC experiments to analyze the crystal unit-cell structures and the isothermal crystallization kinetics of PLLA in biodegradable PLLA-MePEG diblock copolymers. In particular, the effects due to the presence of MePEG that is chemically connected to PLLA as well as the PLLA crystallization temperature T_C are examined.

From the WAXD analysis, both the PLLA and MePEG crystal unit-cell structures are not affected by the chain-connectivity as well as the block ratio between PLLA and MePEG. These structural parameters are also independent of T_C, as expected. With the aid of DSC, we observe that the equilibrium melting temperature of PLLA in the diblock samples decreases dramatically, indicating that this decreasing behavior is not simply due to the decrease in the PLLA molecular weight. The dilution effect caused by the miscible MePEG block connected to PLLA has a greater influence on the crystallization as well as the melting behavior of PLLA. Therefore, the crystallization of PLLA with lower PLLA molecular weight at the same T_C corresponds to a lower degree of supercooling. As a result, the formed PLLA nucleation density as well as the crystallizability of PLLA decreases with decreasing the PLLA molecular weight. While at lower crystallization temperature regime in which PLLA crystallizes according to the growth mechanism, the increase of the normalized PLLA crystallinity in the diblocks suggests that the presence of amorphous MePEG connected to PLLA indeed promotes the ability for the PLLA chains to diffuse to the crystallization sites. As described by the crystallization process with a nucleation and growth, both the overall crystallinity and the isothermal crystallization growth rate G of PLLA first increase with T_C and then show a decreasing behavior with a further increase in T_C.

The authors thank P. D. Hong for the useful discussions. This work was supported by the National Science Council of the Republic of China through grant NSC 93-2216-E-002-027.

REFERENCES AND NOTES

1. Biodegradable Polymers as Drug Delivery Systems; Chasin, M.; Langer, R., Eds.; Marcel Dekker: New York, 1990.
2. Degradable Polymers: Principles and Applications; Scott, G.; Gilead, D., Eds.; Chapman & Hall: London, 1995.
3. Handbook of Biodegradable Polymers; Domb, A. J.; Kost, J.; Wiseman, D. M., Eds.; Harwood: Singapore, 1997.
4. Mohammadi-Rovshandeh, J.; Farnia, S. M. F.; Sarbolouki, M. N. J Appl Polym Sci 1998, 68, 1949.
5. Bogdanov, B.; Vidts, A. E.; Schacht, E.; Berghmans, H. Macromolecules 1999, 32, 726.
6. Kim, K. S.; Chung, S.; Chin, I. J.; Kim, M. N.; Yoon, J. S. J Appl Polym Sci 1999, 72, 341.
7. Fujiwara, T.; Miyamoto, M.; Kimura, Y.; Sakurai, S. Polymer 2001, 42, 1515.
8. Kim, J. K.; Park, D. J.; Lee, M. S.; Ihn, K. J. Polymer 2001, 42, 7429.
9. Albuerne, J.; Marquez, L.; Muller, A. J.; Raquez, J. M.; Degee, P. H.; Dubois, P. H.; Castelletto, V.; Hamley, I. W. Macromolecules 2003, 36, 1633.
10. Ho, R. M.; Hsieh, P. Y.; Tseng, W. H.; Lin, C. C.; Huang, B. H.; Lotz, B. Macromolecules 2003, 36, 9085.
11. Chen, W.; Luo, W.; Wang, S.; Bei, J. Polym Adv Technol 2003, 14, 245.
12. Bhattarai, N.; Kim, H. Y.; Cha, D. I.; Lee, D. R.; Yoo, D. I. Eur Polym Mater 2003, 39, 1365.
13. Sun, J.; Hong, Z.; Yang, L.; Tang, Z.; Chen, X.; Jing, X. Polymer 2004, 45, 5969.
14. Shin, D.; Shin, K.; Aamer, K. A.; Tew, G. N.; Russell, T. P.; Lee, J. H.; Jho, J. Y. Macromolecules 2005, 38, 104.
15. Hamley, I. W.; Castelletto, V.; Castillo, R. V.; Muller, A. J.; Martin, C. M.; Pollet, E.; Dubois, P. H. Macromolecules 2005, 38, 463.
16. Gref, R.; Mibamitake, Y.; Peracchia, M. T.; Trubetskoy, V.; Torchilin, V.; Langer, R. Science 1994, 263, 1600.
17. Hu, D. S. G.; Liu, H. J. J Appl Polym Sci 1994, 51, 473.
18. Du, Y. J.; Lemastra, P. J.; Nijenhuis, A. J.; Aert, H. A. M.; Bastiaansen, C. Macromolecules 1995, 28, 2124.
19. Rashkov, I.; Manolova, N.; Li, S. M.; Espartero, J. L.; Vert, M. Macromolecules 1996, 29, 50.
20. Huh, K. M.; Bae, Y. H. Polymer 1999, 40, 6147.
21. Vasanthakumari, R.; Pennings, A. J. Polymer 1983, 24, 175.
22. Nijenhuis, A. J.; Colstee, D. W.; Grijpma, W.; Pennings, A. J. Polymer 1996, 37, 5849.
23. Iannace, S.; Nicolais, L. J Appl Polym Sci 1997, 64, 911.
24. Miyata, T.; Masuko, T. Polymer 1998, 39, 5515.

25. Di Lorenzo, M. L. Polymer 2001, 42, 9441.
26. Abe, H.; Kikkawa, Y.; Inoue, Y. Biomacromolecules 2001, 2, 1007.
27. Tsuji, H.; Miyase, T.; Tezuka, Y.; Saha, S. K. Biomacromolecules 2005, 6, 244.
28. Di Lorenzo, M. L. Eur Polym J 2005, 41, 569.
29. Polymer Data Handbook; Mark, J. E., Ed.; Oxford University Press: New York, 1999.
30. Brizzolara, D.; Cantow, H. J.; Diederichs, K.; Keller, E.; Domb, A. J. Macromolecules 1996, 29, 191.
31. Marcos, J. I.; Orland, E.; Zerbi, G. Polymer 1990, 31, 1899.
32. Hoffman, J. D.; Weeks, J. J Res Natl Bur Stand Sect A 1962, 66, 13.
33. Cebe, P.; Hong, S. D. Polymer 1986, 27, 1183.
34. Holdsworth, P. J.; Turner-Jones, A. Polymer 1971, 12, 195.
35. Avrami, M. J Chem Phys 1940, 8, 212.